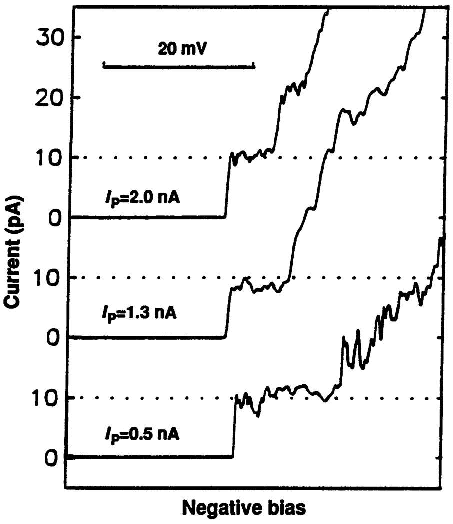

Fig. 5. Current-voltage curves of several devices made from the same heterostructure wafer; I_p gives the value of the peak current, which is a measure of the "electrical size" of a device.

current is limited by the single-electron charging effects. This "Coulomb staircase" behavior is seen better in the magnetotunneling data because B suppresses the short period (~1 mV) modulation. Steps corresponding to from one to six or seven electrons dynamically stored in the well are visible in the data of Fig. 4B.

The calculated values of $I^{(1)}$ are $I^{(1)+} \approx 4$ pA and $I^{(1)-} \approx 11$ pA in the positive and negative polarity, respectively. The experimental values, obtained from the first steps of several devices (Figs. 2 and 5), are $2I^{(1)+} = 9 \pm 2$ pA and $I^{(1)-} = 9.5 \pm 1$ pA; the agreement with the calculated values is very good because the transmission coefficients were obtained by fitting data of a large-area device. Moreover, in the negative bias $T_E >> T_C$ and we can estimate $I^{(1)-}$ as simply the current due to one electron tunneling every $\tau_W \approx \hbar/T_C E_0$: $I^{(1)-} = e/\tau_W \approx 14$ pA, which is also in good agreement with experiment. From the voltage extent of the steps in the negative bias and from fitting of current peaks in the positive bias (*16*) we obtain values of $U_C \approx 20$ K and $\delta E \approx 40$ K that are consistent with the observed temperature dependencies (for example, Fig. 3). Also, the sharpness of the rising current steps [0.2 mV, corresponding to 0.05 meV; see inset in Fig. 2C] is in itself strong evidence for a many-body component (such as U_C) in the tunneling-inhibiting potential, since it is not subject to various broadening mechanisms.

There are three major differences between SET in metal double junctions and in submicrometer DBRTS. First and most obvious is that Coulomb blockade is masked in DBRTS by a large threshold bias $V_{th} \sim 2E_0/e$ needed to align the states in the well with the emitter Fermi energy. Second, the size quantization of the well states in DBRTS coexists with the SET charging so that the two effects may be difficult to separate in measured *I-V* curves. Third, there are no electrons in the well at biases $V < V_{th}$ (zero current), unlike the case of experiments in (*1–4*). This effect is important because the charging energy of addition of the second electron involves two-electron repulsion in the well (*17*) and is greater than U_C for the first electron (*18*).

REFERENCES AND NOTES

1. T. A. Fulton and G. J. Dolan, *Phys. Rev. Lett.* **59**, 109 (1987); L. S. Kuzmin and K. K. Likharev, *JETP Lett.* **45**, 494 (1987); J. B. Barner and S. T. Ruggiero, *Phys. Rev. Lett.* **59**, 807 (1987).
2. C. J. Gorter, *Physica* **17**, 777 (1951); I. Giaever and H. R. Zeller, *Phys. Rev. Lett.* **20**, 1504 (1968).
3. For a review, see D. V. Averin and K. K. Likharev, in *Mesoscopic Phenomena in Solids*, B. L. Altshuler, P. A. Lee, R. B. Webb, Eds. (Elsevier, Amsterdam, 1991).
4. J. H. F. Scott-Thomas, S. B. Field, M. A. Kastner, H. I. Smith, D. A. Antoniadis, *Phys. Rev. Lett.* **62**, 583 (1989); L. P. Kouwenhoven, B. J. van Wees, K. J. P. M. Harmans, J. G. Williamson, *Surf. Sci.* **229**, 290 (1990); U. Meirav, M. A. Kastner, S. J. Wind, *Phys. Rev. Lett.* **65**, 771 (1990).
5. H. van Houten and C. W. J. Beenakker, *Phys. Rev. Lett.* **63**, 1893 (1989); Y. Meir, N. S. Wingreen, P. A. Lee, *ibid.* **66**, 3048 (1991).
6. See, for example, K. Kash *et al.*, *Appl. Phys. Lett.* **49**, 1043 (1986).
7. M. A. Reed *et al.*, *Phys. Rev. Lett.* **60**, 535 (1988).
8. M. Tewordt *et al.*, *J. Phys. Condens. Matter* **2**, 8969 (1990); S. Tarucha and Y. Hirayama, *Phys. Rev. B* **43**, 9373 (1991); M. W. Dellow *et al.*, *Electron. Lett.* **27**, 134 (1991).
9. B. Su, V. J. Goldman, M. Santos, M. Shayegan, *Appl. Phys. Lett.* **58**, 747 (1991).
10. V. J. Goldman, D. C. Tsui, J. E. Cunningham, *Phys. Rev. B* **35**, 9387 (1987); *Phys. Rev. Lett.* **58**, 1256 (1987).
11. A. N. Korotkov, D. V. Averin, K. K. Likharev, *Physica B* **165&166**, 927 (1990); L. I. Glazman and K. A. Matveev, *JETP Lett.* **51**, 484 (1990); A. Groshev, *Phys. Rev. B* **42**, 5895 (1990).
12. V. J. Goldman, D. C. Tsui, J. E. Cunningham, *Solid State Electron.* **31**, 731 (1988); A. Zaslavsky, V. J. Goldman, D. C. Tsui, J. E. Cunningham, *Appl. Phys. Lett.* **53**, 1408 (1988).
13. $C_W = C_E + C_C$. For the device shown in Figs. 2 to 4 at $V = -200$ mV we estimate $C_E \simeq 3 \times 10^{-17}$ F and $C_C \simeq 2 \times 10^{-17}$ F.
14. R. Landauer, *Philos. Mag.* **21**, 863 (1970).
15. C. G. Darwin, *Proc. Cambridge Philos. Soc.* **27**, 86 (1930).
16. B. Su, V. J. Goldman, J. E. Cunningham, in preparation.
17. G. W. Bryant, *Phys. Rev. Lett.* **59**, 1140 (1987).
18. V. J. Goldman, B. Su, J. E. Cunningham, in *Proceedings of the International Symposium on Nanostructures and Mesoscopic Systems*, W. P. Kirk and M. A. Reed, Eds. (Academic Press, New York, 1991).
19. We are grateful to J. E. Lukens for use of electron beam lithography facility and M. Shayegan for DBRTS material used in initial stages of this work (*9*). Supported in part by an Alfred P. Sloan Research Fellowship.

26 September 1991; accepted 9 December 1991

Gas-Phase Rates of Alkane C–H Oxidative Addition to a Transient CpRh(CO) Complex

ERIC P. WASSERMAN, C. BRADLEY MOORE,* ROBERT G. BERGMAN*

The gas-phase irradiation of CpRh(CO)$_2$ (Cp = η^5-C$_5$H$_5$) was examined in order to study the rates of reaction of the 16-electron intermediates presumed to be involved in the C–H oxidative addition of alkanes. "Naked" (unsolvated) CpRh(CO) was detected, and direct measurements of the rates of reaction of this very short-lived complex with alkane C–H bonds were made. Activation of C–H bonds occurs on almost every collision for alkanes of moderate size, and intermediates in which the alkanes are bound to the metal centers, without their C–H bonds being fully broken, are implicated as intermediates in the overall reaction.

"UNACTIVATED" CARBON-HYDROGEN bonds, of the type present in alkanes, are among the strongest single bonds known. Because alkanes and alkyl chains make up a large percentage of natural materials, there is an incentive to develop methods for converting these unactivated C–H bonds into more reactive, and therefore useful, organic functional groups.

Activation of C–H bonds occurs readily on metal surfaces. There are also several known biological systems (such as cytochrome P-450 and methane monooxygenase) that contain metal complexes at their active sites that are capable of selectively activating C–H bonds. Some of these reactions undoubtedly proceed by free radical mechanisms, but it has been thought for some time that others are initiated by insertion of a metal center into the C–H linkage of the alkane R–H in a so-called "oxidative addition reaction." This leads to a hydrido(alkyl)metal complex, R–M–H, as shown in Eq. 1.

$$M + R\text{–}H \rightarrow R\text{–}M\text{–}H \qquad (1)$$

Several years ago we and others (*1, 2*) discovered a group of well-characterized hydrocarbon-soluble organometallic complexes capable of effecting the intermolecular oxidative addition or "C–H bond activation" reaction illustrated in Eq. 1 with sim-

---

Materials and Chemical Sciences Division, Lawrence Berkeley Laboratory, and the Department of Chemistry, University of California, Berkeley, CA 94720.

*To whom correspondence should be addressed.

ple alkanes. These transformations lead to stable, isolable products in which an alkane C–H bond has been broken and new metal-hydrogen (M–H) and metal-carbon (M–C) bonds have been formed. The metal complexes used in this reaction have the general structure $Cp(L)MH_2$ and $CpML_2$, where Cp is an abbreviation for the five-membered ring π-bound ligand η^5-C_5H_5, L represents a carbon monoxide or trialkylphosphine ligand, and the metal M is Ir or Rh. Complexes containing the permethylated analog η^5-C_5Me_5 (Cp*) exhibit the same type of chemistry. Irradiation of these molecules with ultraviolet light causes separation of H_2 or L from the metal center, and in the presence of alkanes (R–H) the intermediates formed in this photochemical reaction lead to complexes of structure Cp(L)M(H)(R).

It is often presumed that "naked" 16-electron CpML and Cp*ML intermediates are involved in these reactions. We report the detection of a transient unsolvated CpML species and direct measurements of the rates of reaction of this type of complex with alkane C–H bonds. The overall C–H activation process occurs at rates close to the gas-kinetic values—that is, on almost every collision—for alkanes of moderate size. The magnitudes of the rates of C–H oxidative addition for various alkanes shed light on the mechanism of C–H activation in both the gas phase and solution.

In addition to evidence implicating short-lived coordinatively unsaturated CpML species in these reactions (*3*), it has become increasingly clear that "solvates" [referred to by various workers as "alkane complexes" (*4*), "σ-complexes" (*5*), or "agostic complexes" (*6*)] are also important as intermediates in these reactions. In noble gas solvents such as liquid Xe and liquid Kr, recent time-resolved infrared flash kinetic studies showed that Cp*Rh(CO) could not be detected directly because it reacts very rapidly to form both noble gas and alkane complexes. The reaction observed directly in this system (7) is the conversion of a spectroscopically detectable (albeit short-lived) Cp*(CO)Rh(alkane) complex to the oxidative-addition product Cp*(CO)Rh(R)(H). At temperatures near −100°C, this reaction proceeds with an activation energy of about 4.5 kcal mol^{-1} for RH = cyclohexane and RH = neopentane.

To provide the presumed initially formed intermediate in the above experiments with a lifetime long enough for it to be detectable with our apparatus, we have switched to the gas phase. Because of its favorable volatility and satisfactory quantum yield for photochemical decomposition, we examined the irradiation of $CpRh(CO)_2$ instead of the pentamethyl-substituted derivative used in the liquid Kr solution studies. The spectrometer and flowing-gas cell used for these experiments, similar to those now in operation in several laboratories (*8*), was a modified version of that described (*9*) in a study of gas-phase substitution reactions of $CpCo(CO)_2$. The irradiations were carried out at 308 nm on samples containing the rhodium dicarbonyl approximately at its vapor pressure (~400 mtorr at 20°C) mixed with a total of 12 to 30 torr of Ar buffer gas containing variable partial pressures of alkane. The energy per pulse used with the laser was ~150 mJ cm^{-2}. The measured rates of reaction with the smallest alkane used here (methane) were somewhat pressure-dependent at total pressures lower than 10 torr. However, above this pressure the rate constants leveled off to values that we presume represent the high-pressure limiting velocities. We therefore believe that the rate constants measured above 10 torr of Ar bath gas for methane (and even lower total pressures for the more vibrationally complex higher alkanes) represent the rates of reaction of species that have undergone collisional deactivation to their ground vibrational levels (*10*).

Upon photolysis of ~400 mtorr $CpRh(CO)_2$ (*11*) (compound **1** in Fig. 1) in Ar at room temperature, initial bleaching of the infrared absorptions at 2003 and 2060 cm^{-1} due to loss of **1** was seen, as was the appearance of a new band peaking at 1985 cm^{-1}. No other strong product bands were observed immediately after photolysis, although weaker bands at 1963 and 2035 cm^{-1} were noted. On the basis of work in matrices (*12*) and in liquid Kr (*7, 13, 14*), it is reasonable that the 1985 cm^{-1} band arises from the unsolvated monocarbonyl CpRh(CO) (compound **2** in Fig. 1). In the absence of alkane, the amplitude of the band due to **2** decays with a half-life of about 1 μs, and a shoulder grows at ~1990 cm^{-1}; this shoulder, along with a band at ~1858 cm^{-1}, is due to the production of the dinuclear adduct **5**. In the presence of H_2, CO, or alkanes (such as in Fig. 2), the 1985 cm^{-1} band decays more rapidly (for example, at 300 mtorr, cyclohexane decay occurs with half-life $t_{1/2}$ = ~250 ns), which leads to the production of absorptions due either to substitution products (in the case of CO) or to oxidative addition products (H_2 and alkanes). Figure 3 illustrates typical transient digitizer traces for the decay of CpRh(CO) in argon-neopentane at 1985 cm^{-1} and the concomitant rise of absorption at 2037 cm^{-1} due to Cp(CO)Rh(neopentyl)(H). The alkyl hydride products appear to be stable over the time scale convenient for measurement in our system ($t_{1/2}$ > 1 ms). This result is consistent with the observations of Perutz and co-workers (*13*), who observed the rate constant for decay of CpRh(CO)(Cy)(H) in CO-free cyclohexane solution to be ~50 s^{-1} (Cy = cyclohexyl) (*15*).

The data in Table 1 summarize the rate constants measured for the reaction of CpRh(CO) with CO, H_2, and alkanes, along with isotopically substituted molecules D_2 and CD_4. Use of the hard-sphere collision rates calculated for the various reactive gases examined in this study allows us to estimate the efficiencies for reaction of CpRhCO (Table 1). The most dramatic aspect of these data is that all of the rates are within an order of magnitude of the calculated gas-kinetic values. Therefore, reactions occur (even in the case of H–H and C–H

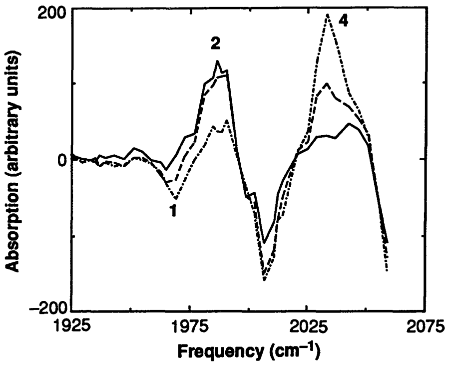

Fig. 2. Transient absorption spectra illustrating the reaction of **2** with 0.3 torr *c*-C_6H_{12} in 28 torr Ar. Solid line, 0.2 μs after photolysis; dashed line, 0.4 μs after photolysis; dotted-dashed line, 0.6 μs after photolysis.

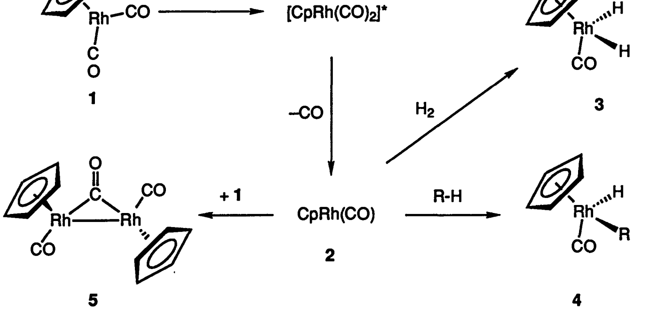

Fig. 1. Photolysis of $CpRh(CO)_2$.

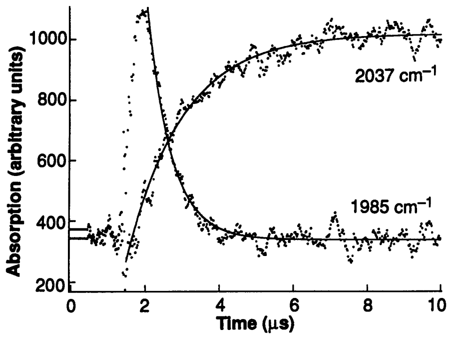

Fig. 3. Transient absorption traces taken at 1985 and 2037 cm^{-1} that follow the decay of CpRh(CO) and the formation of Cp(CO)Rh-[$CH_2C(CH_3)_3$](H), respectively, from the reaction of CpRh(CO) with neopentane. Pressure of gases: 12.6 torr Ar and ~0.08 torr neopentane. The shock wave transients were removed from these traces.

oxidative addition) on nearly every collision. The gradually increasing rates (and calculated reaction efficiencies) for the alkanes are reminiscent of results reported in a recent study by Rayner and co-workers (*16*), who found that gas-phase equilibrium constants for the reaction of alkanes with $W(CO)_5$ (where C–H oxidative addition does not occur, so interaction of the W center and the hydrocarbon stops at the alkane-complex stage) also increased with increasing alkane size (*17*).

We propose the reaction coordinate diagram in Fig. 4 to account for both the rapid rates of reaction measured here and the ~4.5 kcal mol^{-1} barrier observed for the conversion of cyclohexane and neopentane complexes to alkyl hydrides, measured in liquid Kr (7). As one follows the reaction path from left to right, the system passes from the separated reactants to a pair of potential wells. The first well represents the energy of the σ-type alkane complex postulated earlier (7), and the second is the alkyl hydride Rh(III) C–H oxidative addition product. The >15 kcal mol^{-1} exothermicity of the reaction is a rough estimate based on the minimum lifetime of the product Cp(CO)Rh(R)(H). In this view of the reaction mechanism, the 4.6 kcal mol^{-1} barrier measured in our liquid Kr experiments is that associated with movement from the first well to the second. On the basis of the work of Rayner and others (*16, 17*), we chose −10 kcal mol^{-1} as a conservative estimate of the enthalpy of alkane-metal binding in the cyclohexane and neopentane complexes illustrated as CpRh(CO)···(R–H) in Fig. 4.

Table 1. Rate constants for reactions of CpRh(CO).

Reactant	k_{obs} (10^{10} cm^3 s^{-1} per molecule)*	Efficiency†
CO	1.5 ± 0.3	0.43
H_2	1.6 ± 0.3	0.17
D_2	1.6 ± 0.7	0.22
CH_4	0.58 ± 0.26	0.14
CD_4	0.47 ± 0.10	0.11
C_2H_6	1.8 ± 0.5	0.49
$C(CH_3)_4$	2.1 ± 0.6	0.60
c-C_6H_{12}	2.8 ± 0.9	0.82

*All rate constants were calculated by averaging at least 20 runs; errors are the SD of these independent measurements. †Fraction of gas-kinetic value.

The first stage of the reaction is the formation of a collision complex between CpRhCO and the alkane. In the experimentally demonstrated high-pressure limit, this complex undergoes vibrational deactivation at approximately the gas-kinetic collision rate (about 9 × 10^7 s^{-1} at 10 torr Ar), and little redissociation of the initially formed, vibrationally excited alkane complex to CpRhCO and free alkane occurs. In the liquid (7), where the collisional and therefore vibrational stabilization time scale is some five orders of magnitude faster than those in the gas-phase experiments at the pressures reported here (*18*), the complex is stabilized much more rapidly than the C–H activation product Cp(CO)Rh(R)(H) is formed unimolecularly. This would happen in the gas phase if the transition state between complex and product was sufficiently tight that thermal activation would overcome the barrier to form the product. However, because the initial energy of the reactants is well in excess of the barrier to products, if the transition state is loose the product may be formed directly and be the primary initial result of vibrational stabilization. In either case, at pressures sufficient to cause vibrational deactivation of the initial rhodium-alkane complex, formation of the complex is the rate-determining step of the reaction. If there is little or no barrier to this initial reaction step (which seems reasonable), the overall process may occur at or near the gas-kinetic rate, as we observe.

Because alkane complex formation is an exothermic reaction with a very low barrier, the forward rate k_f should have an extremely early or "loose" transition state. It is not surprising, therefore, that these rates do not correlate with energies associated with complete cleavage of the C–H bond, such as bond dissociation energy or acidity, and it is also reasonable that very small isotope effects should be observed. The modest increase in rates of association with increasing molecular size may be due to an increasing long-range attractive interaction between the reactants, or the increase may be a consequence of the fact that our hard-sphere collision frequency calculations are inevitably somewhat approximate. In any case, the magnitude of the binding energy between CpRhCO and molecules such as cyclohexane and neopentane (at least 5, and probably more nearly 10 kcal mol^{-1}) is larger than can be accounted for by van der Waals forces. The effect therefore requires some type of bonding interaction between the metal center and the alkane, probably through the C–H bonds in the manner of the now well-established strong interaction between metal centers and H_2 in so-called "dihydrogen complexes" (*19*). Resolution of these questions awaits future theoretical studies and dynamics experiments as well as attempts to prepare and isolate alkane complexes and study them directly.

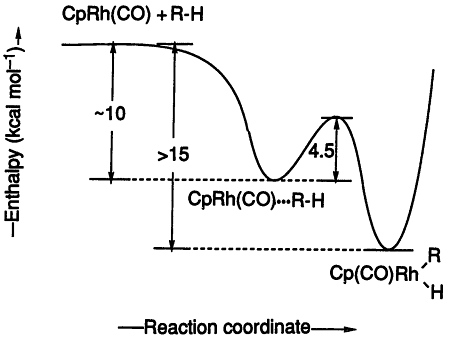

Fig. 4. Proposed reaction coordinate diagram for the gas-phase reaction of CpRh(CO) with alkane R–H to give oxidative addition product Cp-(CO)Rh(R)(H). Estimated energy differences are based on both solution and gas-phase determinations (see text).

REFERENCES AND NOTES

1. A. H. Janowicz and R. G. Bergman, *J. Am. Chem. Soc.* **104**, 352 (1982); J. K. Hoyano and W. A. G. Graham, *ibid.*, p. 3723; A. H. Janowicz and R. G. Bergman, *ibid.* **105**, 3429 (1983).
2. For reviews on this subject, see E. L. Muetterties, *Chem. Soc. Rev.* **12**, 283 (1983); A. E. Shilov, *Activation of Saturated Hydrocarbons by Transition Metal Complexes* (Reidel, Dordrecht, Holland, 1984); R. G. Bergman, *Science* **223**, 902 (1984); R. H. Crabtree, *Chem. Rev.* **85**, 245 (1985); J. Halpern, *Inorg. Chim. Acta* **100**, 41 (1985).
3. See (*1*) and J. M. Buchanan, J. M. Stryker, R. G. Bergman, *J. Am. Chem. Soc.* **108**, 1537 (1986); R. A. Periana and R. G. Bergman, *ibid.*, p. 7332; C. K. Ghosh and W. A. G. Graham, *ibid.* **109**, 4726 (1987); W. D. Jones and F. J. Feher, *ibid.* **106**, 1650 (1984); *Acc. Chem. Res.* **22**, 91 (1989).
4. Z. H. Kafafi, R. H. Hauge, J. L. Margrave, *J. Am. Chem. Soc.* **107**, 6134 (1985).
5. R. A. Periana and R. G. Bergman in (*3*); R. M. Bullock, C. E. L. Headford, K. M. Hennessy, S. E. Kegley, J. R. Norton, *ibid.* **111**, 3897 (1989).
6. For reviews, see M. Brookhart and M. L. H. Green, *J. Organomet. Chem.* **250**, 395 (1983); R. H. Crabtree in (*2*).
7. B. H. Weiller *et al.*, *J. Am. Chem. Soc.* **111**, 8288 (1989).
8. For reviews of recent progress in this area, see K. Schaffner and F. W. Grevels, *J. Mol. Struct.* **173**, 51 (1988); E. Weitz, *J. Phys. Chem.* **91**, 3945 (1987); M. Poliakoff and E. Weitz, *Adv. Organomet. Chem.* **25**, 277 (1986); Y. Ishikawa, P. A. Hackett, D. M. Rayner, *J. Mol. Struct.* **174**, 113 (1988); B. H. Weiller and E. R. Grant, in *Gas Phase Inorganic Chemistry*, D. H. Russell, Ed. (Plenum, New York, 1987), pp. 227–244.
9. E. P. Wasserman, R. G. Bergman, C. B. Moore, *J. Am. Chem. Soc.* **110**, 6076 (1988).
10. In the reaction of CH_4 with CpRh(CO), for exam-

ple, the quantity $k_{obs}/[CH_4]$ (k_{obs}, observed rate) was not affected by the total pressure under conditions in which the total pressure was >10 torr. These relatively complex molecules relax somewhat more efficiently than Group VI metal carbonyls: Compare with P. L. Bogdan, J. R. Wells, E. Weitz, *ibid.* **113**, 1294 (1991).
11. E. O. Fischer and K. Bittler, *Z. Naturforsch. B* **16**, 225 (1961).
12. A. J. Rest, I. Whitwell, W. A. G. Graham, J. K. Hoyano, A. D. McMaster, *J. Chem. Soc. Chem. Commun.* **1984**, 624 (1984); *J. Chem. Soc. Dalton Trans.* **1987**, 1181 (1987); D. M. Haddleton, *J. Organomet. Chem.* **311**, C21 (1986); R. R. Andrea, H. Luyten, M. A. Vuurman, D. J. Stufkens, A. Oskam, *Appl. Spectrosc.* **40**, 1184 (1986); R. R. Andrea, M. A. Vuurman, D. J. Stufkens, A. Oskam, *Recl. Trav. Chim. Pays-Bas* **105**, 372 (1986).
13. D. M. Haddleton and R. N. Perutz, *J. Chem. Soc. Chem. Commun.* **1985**, 1372 (1985); ______, S. A. Jackson, R. K. Upmacis, M. Poliakoff, *J. Organomet. Chem.* **311**, C15 (1986); S. T. Belt *et al.*, *J. Chem. Soc. Chem. Commun.* **1987**, 1347 (1987); S. B. Duckett *et al.*, *Organometallics* **7**, 1526 (1988).
14. S. T. Belt, F. W. Grevels, W. E. Klotzbuecher, A. McCamley, R. N. Perutz, *J. Am. Chem. Soc.* **111**, 8373 (1989).
15. Greater rates were seen when CO was present.
16. C. E. Brown, Y. Ishikawa, P. A. Hackett, D. M. Rayner, *J. Am. Chem. Soc.* **112**, 2530 (1990); see also Y. Ishikawa, C. E. Brown, P. A. Hackett, D. M. Rayner, *Chem. Phys. Lett.* **150**, 506 (1988).
17. Other workers also find that binding energies for charge-neutral metal-alkane complexes lie in this range. See, for example, G. K. Yang, K. S. Peters, V. Vaida, *Chem. Phys. Lett.* **125**, 566 (1986); J. K. Klassen, M. Selke, A. A. Sorensen, *J. Am. Chem. Soc.* **112**, 1267 (1990).
18. For studies of the rate of vibrational relaxation of coordinatively unsaturated metal carbonyls in solution, see M. Lee and C. B. Harris, *J. Am. Chem. Soc.* **111**, 8963 (1990); S.-C. Yu, R. Lingle, Jr., J. B. Hopkins, *ibid.* **112**, 3668 (1990).
19. For reviews, see G. J. Kubas, *Acc. Chem. Res.* **21**, 120 (1988); *Comments Inorg. Chem.* **7**, 17 (1988).

20. Supported by the Director of the Office of Energy Sciences, Chemical Sciences Division, of the U.S. Department of Energy under contract DE-AC03-76SF00098.

7 August 1991; accepted 17 October 1991

Oxygen Supersaturation in Ice-Covered Antarctic Lakes: Biological Versus Physical Contributions

H. CRAIG, R. A. WHARTON, JR., C. P. MCKAY

Freezing in ice-covered lakes causes dissolved gases to become supersaturated while at the same time removing gases trapped in the ablating ice cover. Analysis of N_2, O_2, and Ar in bubbles from Lake Hoare ice shows that, while O_2 is ~2.4 times supersaturated in the water below the ice, only 11% of the O_2 input to this lake is due to biological activity: 89% of the O_2 is derived from meltwater inflow. Trapped bubbles in a subliming ice cover provide a natural "fluxmeter" for gas exchange: in Lake Hoare as much as 70% of the total gas loss may occur by advection through the ice cover, including ~75% of the N_2, ~59% of the O_2, and ~57% of the Ar losses. The remaining gas fractions are removed by respiration at the lower boundary (O_2) and by molecular exchange with the atmosphere in the peripheral summer moat around the ice.

LAKE HOARE IS ONE OF A NUMBER of ice-covered polar lakes in the Dry Valley Region of southern Victoria Land, Antarctica (*1*) that exist by the grace of two special and regional features: (i) the Transantarctic Mountain Range that blocks the flow of ice from the polar plateau and at the same time effectively eliminates precipitation, and (ii) the very low mean air temperature (~−20°C) that provides permanent ice covers 3 to 6 m thick, sheltering "warm-water" (~0°C) lakes over a region of some 5000 km^2. These lakes lie on the land like a series of Szilardian chemostats, fed by glacial meltwaters of varying nutrient contents and hosting rich benthic and planktonic microflora, all thriving on the unique substandard ecologies of low-light, near-freezing, highly oxygenated waters while shielded by ice from the Antarctic rigors. The uniqueness of these ecological characteristics and of the mechanisms of atmospheric gas exchange and high supersaturation of the water make these Antarctic lakes interesting for studies of both terrestrial and possible early Martian habitats (*2, 3*).

Lake Hoare (*2*) is an elongate (4.1 by 1.0 km), shallow (maximum and mean depths: 34 and 14.2 m) lake at the eastern end of Taylor Valley, fed during austral summer by melt streams from Suess Glacier and Lake Chad. The perennial ice cover, ~5 m thick at the time of our work, melts along the marges during summers to provide a moat ~3 m wide that receives the inflowing water: water is removed entirely by sublimation and ablation of the ice cover and evaporation from the moat (moat area is ~2% of total lake area). The lake water is highly supersaturated in O_2 and N_2, and Wharton *et al.* (*2, 3*) originally proposed that freezing of the lake water produces the N_2 supersaturation but that biological production is the major source for supersaturation of O_2. In this report we show how measurements of N_2 and Ar can be used to evaluate the physical and biological effects responsible for supersaturation of O_2 and the removal rates of gases from lakes by ice convection. This approach is an extension of methods used to evaluate O_2 supersaturation effects in the North Pacific gyres (*4*).

The concentration of dissolved O_2 (Fig. 1) is very high in the well-mixed layer below the ice-water interface, averaging 2.4 times saturation relative to atmospheric solubility: below this layer O_2 decreases rapidly to zero in the bottom water (*2*). O_2 is supplied to the lake by inflowing summer meltwater and by photosynthesis below the ice and is removed by (i) ablation and sublimation of ice containing trapped air bubbles, (ii) respiration, and (iii) molecular exchange in the summer moat around the ice cover. Between these sources and sinks two processes are interposed: enrichment of the dissolved O_2 concentration by the formation of ice at the lake surface, and downward transport of O_2 by diffusion to a respiration sink (algal mats) on the bottom. The O_2 sources have been estimated only indirectly: Wharton *et al.* (*2*) used the sedimentation rate of carbon in a nearby lake and an estimate of the O_2 supplied by stream input to calculate that 69% of the net input of O_2 is due to biological production. These authors (*3*) also used the N_2 and O_2 saturation ratios to calculate the proportions of biological to physical O_2 production: that method gave the fraction of biological input as 68% (*5*). We show, however, that those estimates are an order of magnitude too high because of the use of N_2, rather than Ar, as a surrogate inert gas for O_2.

We analyzed the gases in bubbles trapped in the ice cover. Our measurements were made on vertically oriented elongate bubbles near the upper surface of a block of ice collected during the 1987–1988 field season. Bubbles from three pieces were analyzed by gas chromatography (GC) (*4*) for N_2, O_2, and Ar after crushing and extraction of gases in vacuum (*6*). The results are set out in Table 1.

The most striking observation is that the gases do not resemble air: they are depleted in N_2 and enriched in O_2 and Ar, so that the composition is much more similar to that of dissolved gases in water. The bubble compositions are reasonably uniform, and all values lie between air and solubility compositions. The N_2/Ar ratios are intermediate between that of air (83.6) and that of saturated water at 0°C (37.0), as expected for partitioning of gases between bubbles and water when gas exsolution is occurring as a result of removal of water by freezing. The

H. Craig, Isotope Laboratory, Scripps Institution of Oceanography, University of California at San Diego, La Jolla, CA 92093.
R. A. Wharton, Jr., Desert Research Institute, University of Nevada System, Reno, NV 89506.
C. P. McKay, Space Science Division, National Aeronautics and Space Administration Ames Research Center, Moffett Field, CA 94035.